



Water-tightness Airborne Detection Implementation

D.3.4 – Assessment tests and preliminary data report.

Authors:

**de Badts E (GG), Sanchis Muñoz J (GG), Barba Polo J (GG), Frédéric Y-M (ONERA),
Chatelard C (ONERA), Krapez J.-C (ONERA), Mazel C (AM)**

30 March 2018

Technical references

Project Acronym	WADI
Project Title	Water-tightness Airborne Detection Implementation
Project Coordinator	Elena Gaboardi, youris.com (YOURIS) elena.gaboardi@youris.com, alice.deferrari@youris.com
Project Duration	October 2016 – March 2020 (42 months)
Deliverable No.	D.3.4
Dissemination level*	PU
Work Package	WP 3 - Demonstration of Airborne Innovative Techniques
Task	T3.3 - Onboard UAV sensors system
Lead beneficiary	11 (GG)
Contributing beneficiary/ies	2 (ONERA), 3 (AM), 7(NTGS)
Due date of deliverable	31 March 2018
Actual submission date	

PU = Public

PP = Restricted to other programme participants (including the Commission Services)

RE = Restricted to a group specified by the consortium (including the Commission Services)

CO = Confidential, only for members of the consortium (including the Commission Services)



This project has received funding from the European Union's Horizon 2020 research and innovation programme under grant agreement No 689239.

v	Date	Beneficiary	Author
1.0	05/03/2018	GG	Erik de Badts (GG), Javier Sanchis Muñoz (GG), Juan Barba Polo (GG)
1.0	05/03/2018	ONERA	Frédéric Y-M, Chatelard C, Krapez J.-C
1.0	05/03/2018	AM	Mazel Christophe
1.0	26/03/2018	youris.com	Elena Gaboardi, Veronica Meneghello



Disclaimer

This project has received funding from the European Union's Horizon 2020 research and innovation programme under grant agreement No 689239.

The sole responsibility for the content of this report lies with the authors. It does not necessarily reflect the opinion of the European Union. The European Commission is not responsible for any use that may be made of the information contained therein.

Executive Summary

The use of remotely piloted aircraft systems (RPAS) in remote sensing has particular benefits regarding the immediate deployment, the high resolution of the acquired images derived from low altitude flights, the possibility of flying even in bad weather conditions (clouds) and the relatively low cost of the flights.

A multirotor UAV has been especially designed and manufactured to carry two sensors, a five bands multispectral imager and a thermal infrared (TIR) uncooled imager. Two design iterations have resulted in a flight configuration that permits an acceptable flight time while maximizing flight safety. The new RPA has been tested focusing mainly on its flight performance while bearing the desired payload aboard. During the test the flight parameters have been monitored through a telemetry link in the same operational way as in a real flight mission. Dealing with the aircraft performance, as far as the computer simulations only portrayed its flight in ideal conditions, the test flights aim was to gauge the aircraft flight performance as well as the payload in real conditions.

The aim of this testing phase is to assess that the payload integration and the RPAS final flight configuration fulfills the project objective of developing a RPAS water leak detection in water transportation infrastructures surveillance service. A multicopter is not a flight platform aerodynamically efficient but a static, quasi-static or low speed oriented flight platform. The main concerns about this kind of flight configuration is to achieve the requirements for a good imagery acquisition and then a good detection capability having the possibility of selecting the flight altitude (limited by the legal regulatory frame) monitoring and controlling the whole process from a ground station.

Table of Content

1	Preface.....	1
2	Preliminary aircraft calculation and performance simulation tests.....	2
2.1	Objective	2
2.2	Flight platform fixed parameters	2
2.2.1	Aircraft frame and fly conditions.....	2
2.2.2	Battery pack.....	3
2.2.3	Propellers	3
2.2.4	Motors and electronic speed controllers (ESC) calculation	3
2.3	Flight platform performance simulation results.....	5
2.3.1	Battery simulated performance	6
2.3.2	Motors simulated performance	7
2.3.3	Total drive	8
2.3.4	Multicopter maximum ratings.....	9
3	Telemetry and ground segment trials	12
3.1	Ground segment.....	12
3.2	Telemetry	13
3.3	Cameras' monitoring and control from the GCS.....	14
4	Photogrammetric mission planning	15
4.1	Area selection	15
4.2	Preflight considerations.....	16
4.2.1	Sensors features and constraints	16
4.2.2	Image overlap	17
4.3	Mission planning.....	18
5	Flight performance at field.....	23
5.1	Flight procedure and warning situations	23
5.2	Flight performance during the two test flights.....	24
5.3	Relevant incidents occurred during other flights of the aircraft.....	25
6	Preliminary data analysis	26
6.1	Photogrammetric software	26



6.2	Processing quality report	28
6.3	Generated orthomosaic	30
6.4	Sample indices.....	31
7	Conclusions	34
8	References	35

List of Acronyms

AGL	Above Ground Level
AMSL	Above Mean Sea Level
ASL	Above Sea Level
ESC	Electronic Speed Controller
GCP	Ground Control Point
GCS	Ground Control Station
GSD	Ground Sample Distance (spatial resolution)
IMU	Inertial Measurement Unit
IR	InfraRed
LWIR	Long Wave InfraRed ([8.0-12.0 μm] wavelength)
SMC	Soil Moisture Content
MSL	Mean Sea Level
NDVI	Normalized Difference Vegetation Index
RSSI	Received Signal Strength Indicator
SWIR	Short Wavelength InfraRed ([1.0-2.5 μm] waveband)
S/N	Signal to Noise ratio
UAV	Unmanned Aerial Vehicle
RPAS	Remotely Piloted Aircraft System
TIR	Thermal InfraRed
VNIR	Visible and Near InfraRed ([0.4-1.0 μm] waveband)
WP.n	Work Package n
D.n	Deliverable n
DEM	Digital Elevation Model
DSM	Digital Surface Model
GNSS	Global Navigation Satellite System

1 Preface

WADI is a H2020 funded project (Grant Agreement No. 689239) aimed at developing an airborne water leak detection surveillance service in water transportation infrastructures. The project relies on an innovative concept of coupling and optimizing off-the-shelf optical remote sensing devices and their application on two complementary aerial platforms - manned and unmanned. These platforms are used for distinctive purposes in infrastructure performance observation, i.e.: long distance and strategic infrastructure monitoring, and difficult and/or dangerous areas observation.

The current deliverable D3.4 "Assessment tests and preliminary data report" belongs to Work Package 3 viz. "*Demonstration of Airborne Innovative Techniques*", which primary aim is to provide all elements necessary for the airborne operational environment demonstration of the WADI concept at the two pilot sites of the project (WP5 and WP6).

Water leaks induce soil moisture and /or anomalous vegetation growth, which affect the typical physical effects in terms of darkening surface, surface temperature, thermal inertia soil behavior, and vegetation characterization. The associated physical parameters (i.e. reflectance and temperature) can be extracted from the images acquired in particular spectral ranges. The temperature is measured in the thermal infrared (TIR) spectral range. The other parameters require measurements in the visible and near-infrared spectral ranges. The deliverable D3.1 stated the optimal detection wavelengths.

Under this WP, the most suitable existing (off-the-shelf) cameras operating at the defined wavelengths have been selected and purchased. Other components necessary for the system airborne use, such as on-board computing, inertial platform, and integration console, have been defined and supplied. The selected cameras will be adapted/ integrated/ validated on the manned and the UAV platforms. The proposed in-flight validation will result in the availability of an instrumented platform, and will provide preliminary data measurements for the data processing task (WP4).

Deliverable D3.4 specifically refers to the outcome of Subtasks 3.3.2, as detailed below.

Subtask 3.3.2 *UAV system assessment tests and validation flight*. The UAV flight test system will be conducted including the specific test of remote monitoring system and on board record data system. Gathering some preliminary measurements will be also achieved in order to provide initial data.

The report preparation has been coordinated by GG, with key content inputs from ONERA and with active collaboration from AM.

2 Preliminary aircraft calculation and performance simulation tests for UAV platform

The design of a multirotor aircraft is slightly different from any other fixed or rotary wing flight platform. The main concern in this kind of flying platforms is not the aerodynamic efficiency of the aircraft but the capability of performing static and low speed hovering flights. The low speed hovering capability is essential to carry out image acquisition missions, especially at low altitudes. The imaging systems aboard a small size UAV use to have fixed focal distance. That said, the resolution increases inversely with altitude. The lower the altitude, the higher the image resolution. Unfortunately, a decrease in altitude must be accompanied by an increase of the shutter speed or a decrease of the aircraft speed in order to avoid the image blurring associated with an insufficient shutter speed.

2.1 Objective

The aim of this section is the aircraft calculation in first instance and the simulation of the aircraft flight performance in second instance. The design of a multirotor requires fixing certain parameters like the number of rotors or the frame size. All the calculations and simulations have been carried out with *xcopterCalc*, a flight platform calculator and flight performance simulator written by Markus Müller [1].

2.2 Flight platform fixed parameters

2.2.1 Aircraft frame and fly conditions

The selected flight platform is a four rotor multicopter (quadcopter) in X flying configuration looking for minimizing weight as the main concern in multirotor platforms, and taking into account the well-known excellent flight performance of this flight platform. The size of the frame has been fixed in order to have the possibility of using propellers up to 18 inches. It is important to mention that the propellers' efficiency increases with its size. Although there is also the maneuverability of the aircraft criteria to take into account when selecting the propellers' size. The angular speed of the propeller is inversely proportional to the length of the propeller. The maneuverability decreases proportionally to the propeller length increase. A standard field elevation, air temperature and air pressure has been selected in order to simulate the flight performance of the aircraft.

Number of rotors (simple/coax.)	Frame size (diagonal in mm)	Total weight (with payload) (g)	Flight control unit tilt limit (°)	Field elevation (mASL)	Air temperature (°C)	Air pressure (hPa)
4 (simple)	820	3200	Unlimited	500	25	1013

Table 1. Flight platform fixed parameters.

2.2.2 Battery pack

The dimensioning of the battery pack goes in accordance with the estimated total weight of the flight platform. In this case, a 6S (6 cells of 3.7V in serial configuration giving a total of 22,2V) battery pack has been selected. The capacity of the battery pack must be as large as possible considering that the weight of the battery pack increases with its capacity. In the time of the flight platform design, the most capacity-weight efficient battery pack was the 6S/10000 mAh. Dealing with the maximum discharge rate of the battery pack (C number), until the performance simulation, the best choice is going to be the lowest discharge rate capable battery pack for a question of weight once more.

Type (continuous/max. discharge rate)	Charge status	Configuration	Cell capacity (mAh)	Max. discharge (%)	Internal resistance (Ω)	Cell voltage (V)	C rate (cont./max.)	Cell weight (g)
LiPo 10000 mAh 15/20C	Full	6S1P	10000	85	0.0023	3.7	15/20	207

Table 2. Features of the selected battery pack. The battery parameters are specified for cell, not for pack.

2.2.3 Propellers

The last step for calculating the necessary motors and electronic speed controllers is to select the propellers. After having tested different types of propellers, it has been determined that the safest propeller type was the carbon fiber propellers with T-style fixture (three holes, one for the motor axis and two for the fixing screws). The determination of the number of blades, the diameter and pitch length (measured in inches per revolution) of the propellers has been established after some simulation iterations. The propellers specified in Table 3 assure a good stability and maneuverability together with an acceptable efficiency.

Brand - type	Yoke twist (°)	Diameter (inch)	Pitch (inch)	Number of blades	PConst/TConst	Gear ratio
Custom – T-Style	0	15	5.5	2	1.2/1.0	1:1

Table 3. Propellers' features.

2.2.4 Motors and electronic speed controllers (ESC) calculation

The torque and power of the motors and the continuous and maximum electric power required for the ESCs are calculated by introducing the flight platform, battery pack and propellers' parameters through the wizard calculator of the Figure 1.

Prop-Kv-Wizard

All-up Weight: g

of Rotors:

Frame Size: mm

Battery - Rated Voltage: V

Propeller - Diameter: inch max. 22.7"

Propeller - Pitch: inch max. 9.9"

Propeller - # Blades:

recommended KV: **330 ... 480** rpm/V

min. Motor Power: **475 ... 830** W+

min. ESC size: **25 ... 45** A+

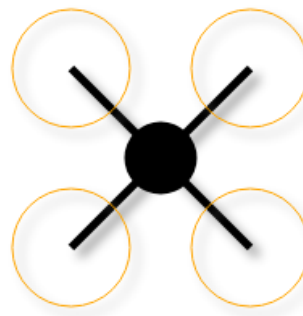


Figure 1. Motor and ESC requirements wizard calculator.

The wizard calculator returns the recommended ranges for motor torque (Kv) and minimum power, and for the minimum current of the ESC.

Manufacturer:

Motortyp:

KV: ... rpm/V

Power Limit: ... W

Weight: ... g

sorted by:

Results: 4

² the production of these motors have been discontinued

	Manufacturer	Motortyp	KV (rpm/V)	Limit (W)	Weight (g)
←	MultiStar	4225-390	390	330	86
←	MultiStar	Elite M4004-400 ²	400	300	91
←	MultiStar	Elite M3508-380 ²	380	320	96
←	MultiStar	4822-390	390	300	98

Figure 2. Matching criteria motor list returned by the wizard calculator.

The best choice is the motor with the highest electrical power limit and the lowest weight considering also the stock availability and the delivery time. The selected motor for the quadcopter is the Multistar 4225-390. Even if the motor maximum electric power is out from the range, the real power demand of each motor is not going to exceed 185W for stability and maneuverability reasons. The simulator states the range (475-830W) assuming full throttle with the maximum payload weight capability of the aircraft. In this case, the

aircraft is under its half weight possible and the throttle is set up to reach maximum throttle at 60% of its capability.

Brand	Type (Kv) - cooling	Kv (torque in rpm/V)	No-load current	Max. electric power (W)	Internal resistance (Ω)	Case length (mm)	Mag. poles	Weight (g)
Multistar	4225(390) - Excellent	390	0.2A@11.1V	330	0.24	25	16	86

Table 4. Features of the selected motor.

The ESC is selected taking into account the current range. The best choice is to select an ESC that is capable of supporting the higher current limit of the range. In this case the higher limit is 45A. Despite the good practice of oversizing the ESC, each motor is not going to exceed 185W/8A. The 40A ESC of the Table 5 has been selected for being largely oversized, for having low weight, for its well-known robustness.

Brand	Model	Current cont./max. in (A)	Internal resistance (Ω)	Weight (g)
Hobbywing	X-Rotor 40A (opto)	40/50	0.003	27

Table 5. Features of the selected ESC.

2.3 Flight platform performance simulation results

Once calculated the motors and the ESCs xcopterCalc simulates the battery, motor, total drive and maximum ratings of the designed aircraft. The xcopterCalc simulator tends to be very conservative. Care must be taken in the interpretation of the simulation results.

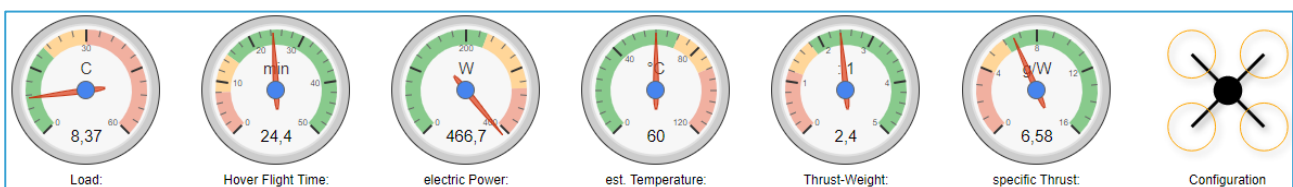


Figure 3. Summary of simulation results.

Figure 3 shows a summary of simulation results. The first clock indicates the maximum load (worst case), that is to say the maximum discharge rate corresponding to the discharge produced by the four motors spinning at maximum electrical power. The selected 6S/10000mAh battery has a continuous discharge rate of 20C where C indicates a current rating (Current = C rating \times Batt. Capacity). That means that the battery can provide 200A (10

Ah x 20 C) continuously until the battery discharge. The hypothetical maximum electrical power consumption is 83,68A (20,92 A x 4 motors, where 20,92 A is the current of one motor at maximum throttle, see Table 7). In this case the maximum battery discharge rate necessary is 8,37C.

The next clock indicates the fly time if the aircraft is just hovering (without linear movement and air currents).

The maximum electrical power of each motor is shown in the third clock. It is important to note that for stability and maneuverability reasons, the real maximum electrical current of each motor is going to be under 6A, that is 3,5 times lower than the maximum electrical current available. To conclude, the real maximum power consumed by each motor is 133,87W, which is largely supported by the 330W motors (it differs from the maximum motor power indicated in Figure 3 and Table 7 because the aircraft is under the half of its weight capability and the maximum real throttle is fixed at 60%).

The fourth clock indicates the temperature that can reach the motor case if the motor is driven to the maximum electrical power. Even at the oversized simulated maximum electrical power, the motor case temperature remains acceptable. It is important to remind that this temperature has been calculated for a maximum electrical power of 466,7W instead of the real 133,87W.

The fifth clock indicates the relation thrust-weight. In this case, the aircraft is capable of a thrust of 2,4 times the weight. The maximum thrust limit of the aircraft is 7,68 kg.

The last clock shows the specific thrust in g/W.

The following sections present the detailed aircraft performance simulations.

2.3.1 Battery simulated performance

Table 6 shows the simulated performance of the battery. This table shows some important parameters as the load, presented in the results summary, the flight time for three different scenarios, the maximum charge used to reach the 85% of the battery discharge specified as parameter for the simulation and the calculated weight. The physical battery weights 160g less than the weight calculated by the simulator.

Battery	
Load:	8.37 C
Voltage:	22.38 V
Rated Voltage:	22.20 V
Energy:	222 Wh
Total Capacity:	10000 mAh
Used Capacity:	8500 mAh
min. Flight Time:	6.1 min
Mixed Flight Time:	17.7 min
Hover Flight Time:	24.4 min
Weight:	1422 g
	50.2 oz

Table 6. Simulated battery performance.

2.3.2 Motors simulated performance

It is not possible to simulate exactly the current consumption profile of a flight as far as it depends from unpredictable parameters like wind, air density, the real propeller efficiency, the planned mission, etc. In order to have a useful flight consumption forecast, it is necessary to establish different current consumption scenarios. In this case, the Table 7 presents the optimal case corresponding to the motors working in its optimum efficiency point, the worst case corresponding to the motors working at maximum electrical power, and the hover case. The current demand of the motors spinning at maximum angular speed is defined by the battery voltage, the KV motor parameter and by the losses introduced by the propeller. That is to say, the revolutions calculated only with the battery voltage and the motors KV parameter refers to the motor working with no-load (no mechanical drag resistance produced by the propeller).

Motor @ Optimum Efficiency	Motor @ Maximum	Motor @ Hover
Current: 5.18 A	Current: 20.92 A	Current: 5.23 A
Voltage: 23.23 V	Voltage: 22.31 V	Voltage: 23.23 V
Revolutions*: 8533 rpm	Revolutions*: 6577 rpm	Revolutions*: 3791 rpm
electric Power: 120.3 W	electric Power: 466.7 W	Throttle (log): 38 %
mech. Power: 106.9 W	mech. Power: 348.6 W	Throttle (linear): 53 %
Efficiency: 88.8 %	Power-Weight: 583.4 W/kg	electric Power: 121.5 W
	264.6 W/lb	mech. Power: 94.2 W
	Efficiency: 74.7 %	Power-Weight: 153.9 W/kg
	est. Temperature: 60 °C	69.8 W/lb
	140 °F	Efficiency: 77.5 %
	Wattmeter readings	est. Temperature: 33 °C
	Current: 83.68 A	91 °F
	Voltage: 22.38 V	specific Thrust: 6.58 g/W
	Power: 1872.8 W	0.23 oz/W

Table 7. Simulated motor performance in three different current consumption scenarios.

The two important parameters of the Motor@Maximum column are the maximum electrical current and the estimated temperature. The rest of the parameters serve as reference when comparing with the Motor@Hover case. By the way, the third column introduces two important parameters to take into account, the minimum throttle for log and linear types. That means, the minimum throttle percentage necessary for letting the aircraft hovering at a static altitude. The lower this parameter is, the lower the aircraft movement latency. A linear throttle between 40% and 60% is okay. Less than 40% makes the aircraft movements too much brusque and can drive to instability. More than 60% makes the aircraft too heavy of movement. A throttle of 50% is perfect for manual transmitters with centered sticks. This way, in manual flight mode, the aircraft is going to hold altitude and hover if the pilot releases accidentally the controls.

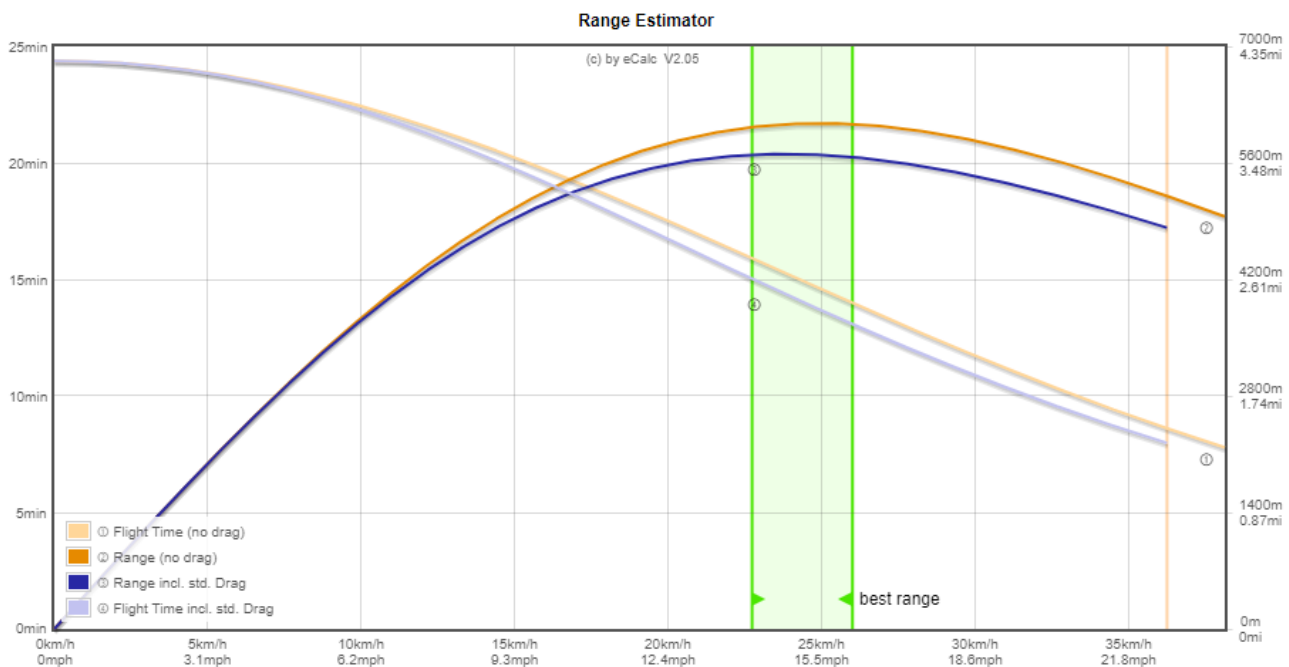


Figure 4. Range estimation based on aircraft speed.

One of the most important simulated parameters is the range together in distance and time, based on the aircraft speed for the ideal case of no drag and for the standard drag case. The best speed range of the calculated aircraft is 23-26 km/h. For 23 km/h, the battery will be discharged at 85% after 15 minutes and a distance of ~5,6 km. At 26 km/h the estimated distance will be almost the same but the battery will reach the 85% of discharge after ~13 minutes. In a real flight, the aircraft doesn't fly at a constant speed so the times vary slightly.

2.3.3 Total drive

The total drive of the aircraft is summarized in the Table 8.

Total Drive	
Drive Weight:	2061 g
	72.7 oz
Thrust-Weight:	2.4 : 1
Current @ Hover:	20.92 A
P(in) @ Hover:	492.4 W
P(out) @ Hover:	376.7 W
Efficiency @ Hover:	76.5 %
Current @ max:	83.66 A
P(in) @ max:	1968.7 W
P(out) @ max:	1394.5 W
Efficiency @ max:	70.8 %

Table 8. Summary of the total drive.

The xcopterCalc simulates the Drive weight (aircraft without payload). In this case, 2061 g indicates that the frame may be heavier than expected (the real total drive weight is ~2,8 kg). The application by the simulator of standard parts' weights instead of the true real weight of each part (motor, ESC, Battery, carbon frame, etc.) introduces this difference. Although the important weight for the performance simulation is the total weight of the aircraft with payload (3,2 kg).

The thrust-weight ratio is an important agility indicator. The bigger, the better. Flying with a thrust-weight ratio of 1,2 or lower is almost impossible.

The total electrical current, the input electrical power, the output mechanical power and the efficiency of the aircraft are shown for the hover and the maximum power cases.

2.3.4 Multicopter maximum ratings

With an all-up total weight of 3,2 kg, the simulator estimates that the aircraft can carry a maximum of additional payload of 3508 g to hover at 80% throttle to guarantee maneuverability (below 50% for aerobatics and below 80% for photography).


Multicopter	
All-up Weight:	3200 g
	112.9 oz
add. Payload:	3508 g
	123.7 oz
max Tilt:	62 °
max. Speed:	40 km/h
	24.8 mph
est. rate of climb:	7.1 m/s
	1398 ft/min
Total Disc Area:	45.60 dm ²
	706.8 in ²
with Rotor fail:	

Table 9. Aircraft maximum ratings.

The theoretically calculated maximum possible tilt angle of the copter to maintain level of flight is 62° (neglecting the down force due to tilt).

The aircraft calculated maximum speed is 40 km/h and the estimated maximum rate of climb is 7,1 m/s.

The total disc area is the area covered by rotors when looking from the top to the copter. The higher the disc area the more efficient the copter gets.

The copter will turn uncontrollable with the fail of one of the motors/rotors.

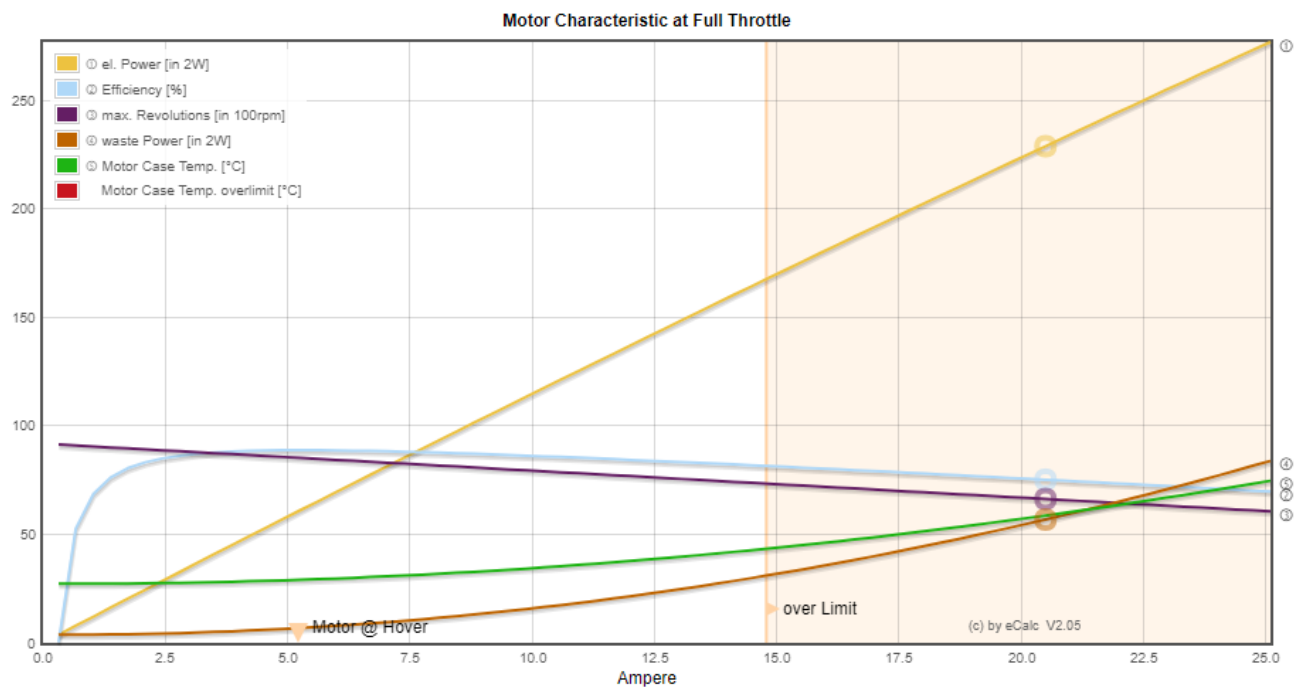


Figure 5. Motor characteristics at full throttle.

Figure 5 shows the motor characteristics at full throttle. Full throttle does not correspond to full power. The full power case is marked with a circle in each characteristic curve. The true over limit, that is the limit of our selected motors is at 14,79A corresponding to 330W which is the maximum electrical power limit of the motors.

The charge of the batteries must be done at a maximum of 1C rate that means at 1C x 10Ah = 10A). For safety reasons, the batteries are always charged at 0,5C / 5A with a SkyRC Q200, which is capable of charging four battery packs at a time at 5A.

The maximum flight time showed by Figure 3 (24,4 min) is calculated for an ideal situation where the battery pack is discharged an 85%. As a safety procedure, the battery pack maximum discharge is 70%, which in ideal conditions corresponds to 20 min of flight time. In real conditions this time decrease to 18 min. As a safety procedure, the maximum flight time must not be greater than 15 min.

For a typical campaign of 8h, taking into account the displacement of the mission home (take-off and landing place), the number of flights will be 10 - 14.

3 Telemetry and ground segment trials

3.1 Ground segment

The designed copter uses the Pixhawk autopilot, the last evolutionary step of the Ardupilot open source project.

Mission Planner is a full-featured ground control station (GCS) for the Ardupilot open source autopilot project.



Figure 6. Ground segment monitoring panel.

Mission Planner can be used as a configuration utility or as a dynamic control supplement for your autonomous vehicle. Here are some functionalities and features of Mission Planner:

- Load the firmware (the software) into the autopilot (APM, PX4...) that controls the autonomous vehicle.
- Setup, configure, and tune the vehicle for optimum performance.
- Plan, save and load autonomous missions into the autopilot with simple point-and-click waypoint entry on Google or other maps.
- Trigger camera based payloads either manually (with a telemetry link) and autonomously.
- Download and analyze mission logs created by the autopilot.
- Interface with a PC flight simulator to create a full hardware-in-the-loop UAV simulator.
- With appropriate telemetry hardware it allows:
 - To monitor the vehicle's status while in operation.
 - To record telemetry logs which contain much more information than the on-board autopilot logs.
 - To view and analyze the telemetry logs.
 - To operate the vehicle in FPV (first person view).

As already said, the GCS Mission Planner is necessary for loading the specific vehicle firmware to the autopilot (flying wing, tricopter, quadcopter, hexcopter, rover, boat, etc.), for configuring the vehicle and for planning the mission. Additionally, if there is a telemetry link available, it allows the mission monitoring and control in real time. The autopilot Pixhawk accepts the modification in flight of most of the configuration parameters like the capacity of the battery, the vehicle speed or the flight mode.

There is no specific trial to do to the ground segment as far as it is used in all the steps of use of the autonomous vehicle.

The Figure 6 shows the monitoring panel of Mission Planner. In the top left corner there is the flight instruments panel with the artificial horizon (pitch indicator), the roll and yaw (compass) indicators, the speed and the climbing rate indicators, as well as some useful specific indicators like the GPS status, the Extended Kalman Filter (used internally for attitude and navigation data fusion) and Vibe warning indicators. The bottom left corner is a fully ground operator customizable multipurpose area. In normal monitoring mode, the operator has a set of numeric indicators. A reference map showing the position and path of the autonomous vehicle occupies the right side of the panel.

3.2 Telemetry

To be able to monitor and control the autonomous vehicle in real time, it is necessary to have telemetry. The telemetry link is composed by an air module wired to the autopilot of the autonomous RPA and ground module connected to the GCS (usually a computer or a tablet).



Figure 7. Air and ground transmitter modules.

Figure 7 shows the two telemetry modules. In Europe, the modules must work in the 433 MHz band with a transmitting power that will not exceed the legal limit of 25 mW.

The telemetry link can be tested in different ways assuming that it is properly configured. The first thing is to check if the GCS connects to the autopilot by pushing the connect button on the top right corner of the GCS monitoring panel. If the connection is successfully, the GCS starts to send all the configuring parameters to the autopilot.

The second thing to do is a range test letting the aircraft on the ground with the telemetry link active and moving away with the GCS maintaining direct and clear vision between the vehicle and the GCS, until the loss of the signal.

The range test can be done while looking to the *Received Signal Strength Indicator (RSSI)* available in Mission Planner (*Initial setup* tab -> *Optional Hardware* -> *Sik Radio*) and shown in the Figure 8.



Figure 8. Sik Radio telemetry link configuration window.

In order to have an estimation of the RSSI signal at signal loss, move away from the aircraft until the signal loss and note the RSSI value.

3.3 Cameras' monitoring and control from the GCS

Monitoring and controlling the cameras from the GCS is useful in inspection, surveillance, audiovisual and first person view applications as in these applications the real time image availability is mandatory. In the frame of this project, the RPAS is used only to drive photogrammetric image acquisition missions. The acquired images need to pass through a preprocessing and processing pipeline for the data become useful. Although both cameras can be monitored from the GCS, it is not practical to do it as it will be necessary to add a shared video link or two dedicated video links for both cameras. This action will increase the total weight and the current consumption, decreasing the maximum flight time.

4 Photogrammetric mission planning

UAVs/RPAS are used in an increasing number of fields and applications. One of the most relevant applications is image acquisition for diverse purposes. In the frame of the project, UAVs are used in water leaks detection surveys. In these surveys, the UAV is used to acquire multispectral and thermal infrared images in order to obtain spectral orthomosaics with photogrammetric grade.

Photogrammetric missions require a good preliminary mission planning considering important parameters like the physical characteristics of the optical systems composing the payload, the flight altitude and speed, the wind, etc.

The aim of the survey trials is to test the designed multicopter together with the integrated payload in real conditions.

4.1 Area selection

The test flights were done on August 11 and October 26, 2017 over a carrot field in the municipality of Villena, an agriculture focused village in the country side of the province of Alicante as be seen in the Figure 9.

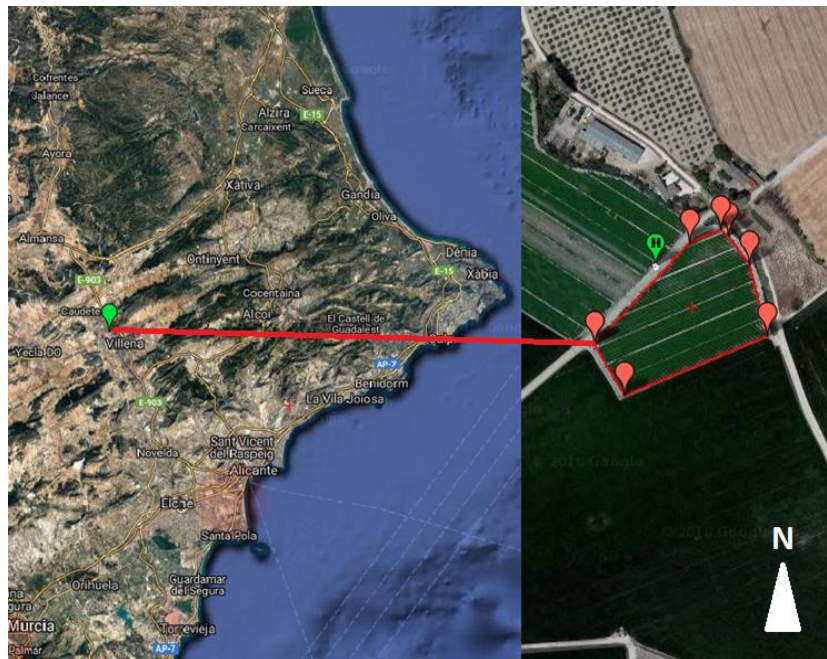


Figure 9. Location of the test field in the municipality of Villena, Alicante.

The carrot's field of the Figure 10 was selected mainly for being an irrigated field where it will be dry and wet areas which will give diverse reflectivity and emissivity dynamic responses over two different dates. Two flight surveys were done two months apart (11/08/2017 and 26/12/2017).

The other important concern about the flight field location is the flight safety. As far as the multicopter is a new specific purpose aircraft, the flight safety must remain a primary concern. The field was chosen for its distance to the closer populated area, which will remain out of the multicopter simulated range.



Figure 10. Test field (carrots) in the municipality of Villena, Alicante.

4.2 Preflight considerations

The photogrammetric mission planning requires adapting the flight to the needs of the specific instrumentation payload.

4.2.1 Sensors features and constraints

The payload is composed of two different cameras with different focal lengths and elementary sensor sizes.

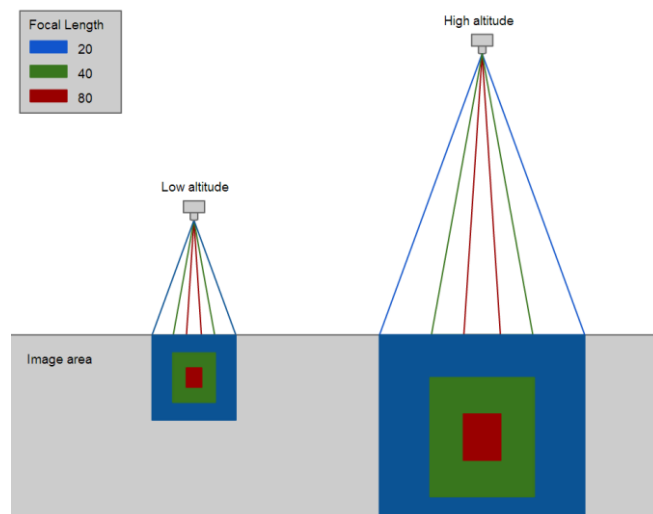


Figure 11. Ground sample distance (GSD) for three focal lengths and two different altitudes.

Figure 11 shows a representation of the ground sample distance (resolution) for three focal lengths and two different altitudes.

The higher the focal length the thinner the field of view and the better the GSD or resolution. A high focal length camera will provide a better resolution while covering less terrain per picture than a camera with a lower focal length. That means that a camera with a high focal length will require more time to cover the same terrain than a camera with a lower focal length.

By the way, for a given focal length, two cameras with different sensor sizes (sensor width and length, the number of pixels will depend on the pixel size) will have different resolutions. The camera with the bigger size sensor (in the sense of number of pixels) will have better resolution while covering the same terrain per picture than the camera with the same focal length but with a smaller number of pixels (for the same total area).

The sensor size of a camera is fixed; it is an unchangeable sensor parameter. Most of the time, the camera focal length in UAV specific cameras is also unchangeable. For these two cases, the only way of increase or decrease the resolution is to select a lower or higher flight altitude as seen in the Figure 11.

The WADI UAV payload is composed of a multispectral Micasense RedEdge 3 camera and a thermal infrared Flir Vue pro R 960 camera. The relevant cameras' features can be found in the D3.3.

4.2.2 Image overlap

The process of point cloud based orthomosaicing method has a common point with the stitching mosaicking method. Both methods require the presence of the same singular image features in successive and side images. Those singular images features are called descriptors. The higher the descriptor's number, the better the point cloud based digital surface model (DSM) and the resulting orthomosaic. To ensure good quality results, an image must have more than one thousand image descriptors common to at least two other images. The more images share a descriptor the better.

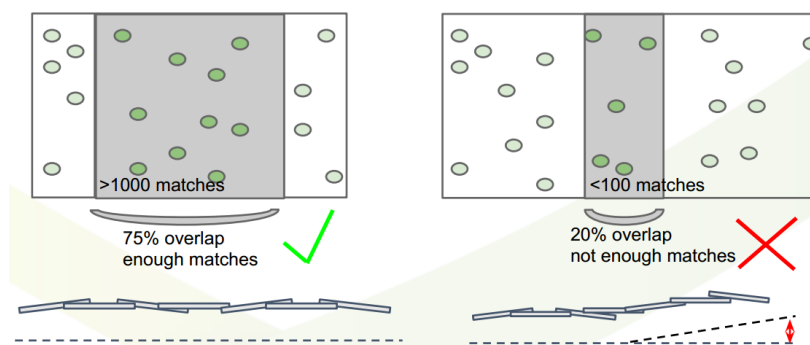


Figure 12. Number of common image descriptors between two images based on its overlap images.

Figure 12 shows two opposite descriptor scenarios. The left side of the picture shows two images with an overlap of 75% that will result in more than 1000 descriptor matches between the two images. On the opposite case is the right side of the picture. The two images have an overlap of 20% resulting in a poor number of descriptor matches.

The overlap must be done between an image and its front, back and side images in order to ensure the generation of a quality DSM. Figure 13 illustrates the concepts of front and side overlap.

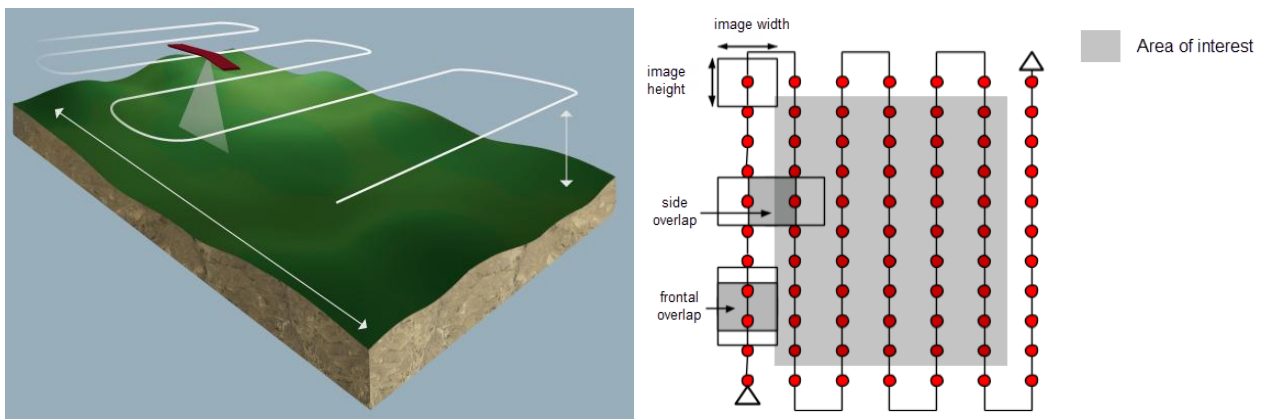


Figure 13. Grid flight path to cover an area of interest.

However, the overlap is unfortunately not the only responsible parameter that affects the number and the quality of the descriptors. The type of photographed surface is a critical parameter to care about. An unsharpened surface like a water mass or a dunes are too smooth to provide a correct number of descriptors between overlapped images. The snow, speed origin blur, geometrical radically changing natural surfaces like trees photographed at a too low altitude, cause the fail of the mosaicking process. See [2] for the internal and external camera parameters definition in Pix4D.

4.3 Mission planning

The first step to plan a photogrammetric mission with a two cameras' based payload is to identify which of the two cameras is more restrictive in terms of focal length, sensor size, and overlapping needs. Calculating and comparing the required altitude to ensure a given GSD in addition to the separation distance between front and side images to meet a specified front and side overlap, will allow to know the most restrictive camera and if the survey must be done in one or more flights.

Prior to any mission planning, the operator must select one of the two parameters, the resolution or the altitude, depending on the needs.

An altitude of 70 m AGL has been set for this mission.

The cameras' performance is analyzed in detail in the following lines.

Micasense RedEdge 3:

As seen in the D3.3, the Micasense RedEdge 3 meets the spectral bands criteria established in the D3.1 prepared in the Task 3.1. The camera has 5 different spectral bands (blue, green, red, red edge and nir) acquired by 5 integrated spare sensors with 5 spare lenses. Each spare camera has a focal length of 5,5 mm, an image size of 1280x960 pixels and a sensor size of 4,8 x 3,6 mm (pixel size calculated from image and sensor sizes). The photogrammetric software, presented later, used for the preprocessing and mosaicking steps, recommends for the case of the Micasense camera, a front overlap of 80% and a side overlap of 60%. With these camera parameters and the altitude of 70 m AGL set by the operator, we calculate the resulting GSD, the distance between shots and the distance between rows. The most restrictive camera will be the one which will have a smaller distance between rows to ensure the correct side overlap.

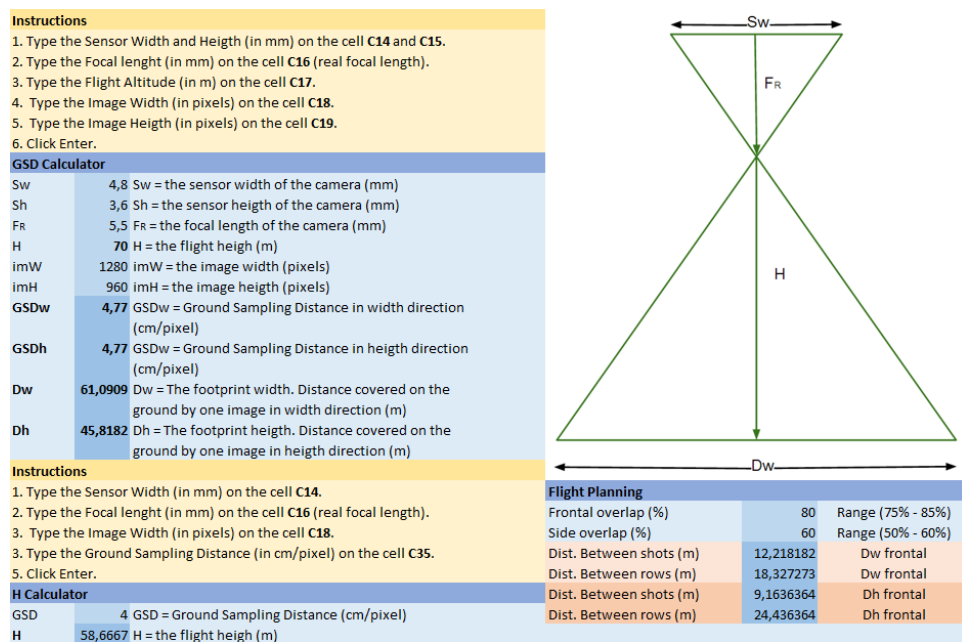


Figure 14. GSD, distance between shots and rows calculated for the Micasense RedEdge 3 flying at an altitude of 70 m AGL.

Figure 14 shows a spreadsheet to calculate the GSD and both distances between shots and between rows based on the camera orientation (the image sensor is rectangular).

Flir Vue Pro R 640:

The Flir Vue Pro R 640 is an uncooled thermal infrared camera. As opposed to the cooled camera used aboard the manned plane, the UAV has a weight limitation that obliges to use uncooled thermal cameras. This model is the best in its class regarding its sensor size and its radiometric capability. The camera has a focal length of 13 mm, an image size of 640x512 pixels and a sensor size of 10,88 x 8,704 mm. For this camera, a front and side

overlap of 90% is recommended by Flir and Pix4D (lower number of pixels, thermal changes between two stripes). As in the previous case, we calculate the resulting GSD, the distance between shots and the distance between rows with the spreadsheet of the Figure 15.

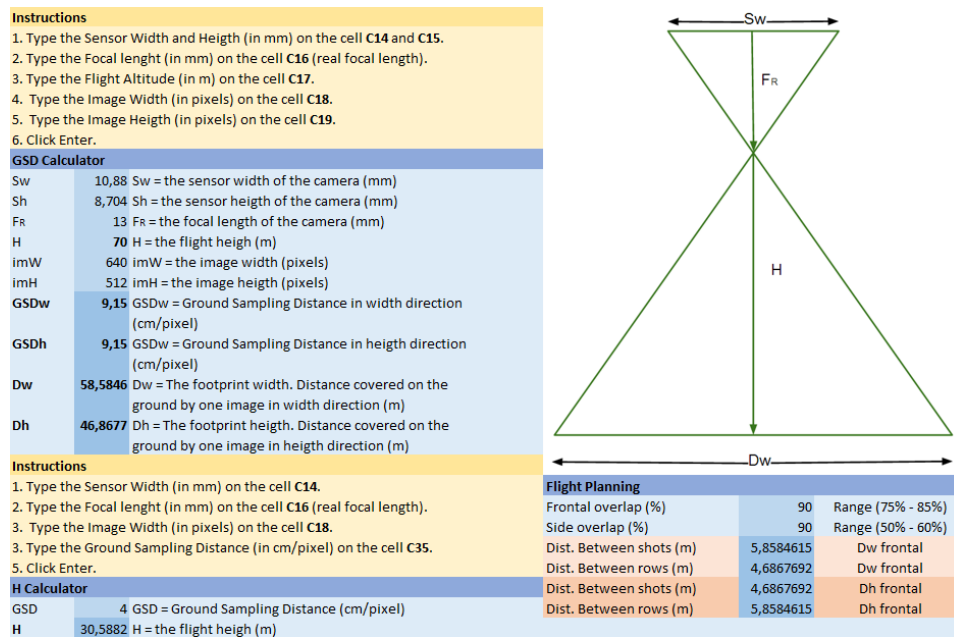


Figure 15. GSD, distance between shots and rows calculated for the Flir Vue Pro R flying at an altitude of 70 m AGL.

Figure 15 shows calculated distances between shots and between rows much smaller than in the case of the Micasense RedEdge 3.

The most restrictive camera is the Flir Vue Pro R 640 as calculated in the Figure 15.

The most restrictive camera is the one that requires the shortest distance between two successive shots and between two stripes. The mission planning must be done according to the most restrictive camera. The GCS has diverse mission planning wizards. The selected wizard is called *Survey Grid* and is shown in the Figure 16.

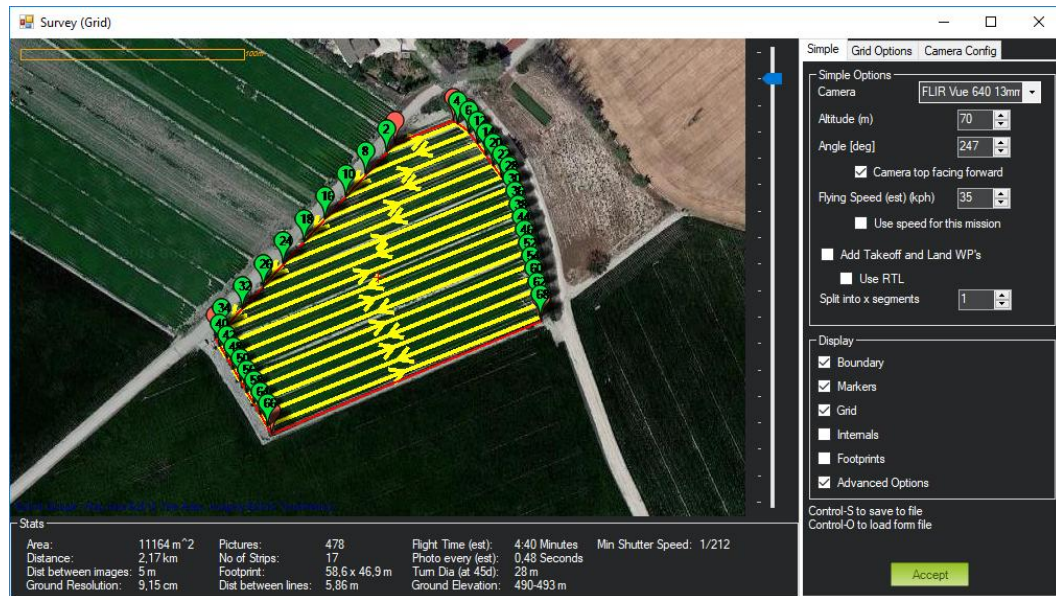


Figure 16. Survey Grid mission planning wizard.

The wizard will setup the necessary flight commands and waypoints to drive the mission by specifying the area of interest, the most restrictive camera parameters, the altitude and the speed of flight among other secondary options.

The stats area at the bottom of the Survey Grid window provides useful and important actual mission information like the total area of the specified area of interest in square meters, the total distance that will fly the UAV to complete the mission, the distance between images (shots), the ground resolution (GSD), the total number of pictures taken, the number of strips (rows), the ground footprint of a picture, the distance between lines (strips, rows), the estimated flight time, the estimated time between shots, the ground elevation or the minimum shutter speed.

The two most important parameters to focus on are the flight time, as far as the approximate flight time (with a given battery) is usually known, and the estimated time between shots.

In Figure 16, we appreciate a time between shots of 0,48s. This is insufficient as the maximum trigger speed of the Flir Vue Pro R is 1s. To meet the camera trigger requirement we step down the aircraft speed until the time between shots of 1s is reached.

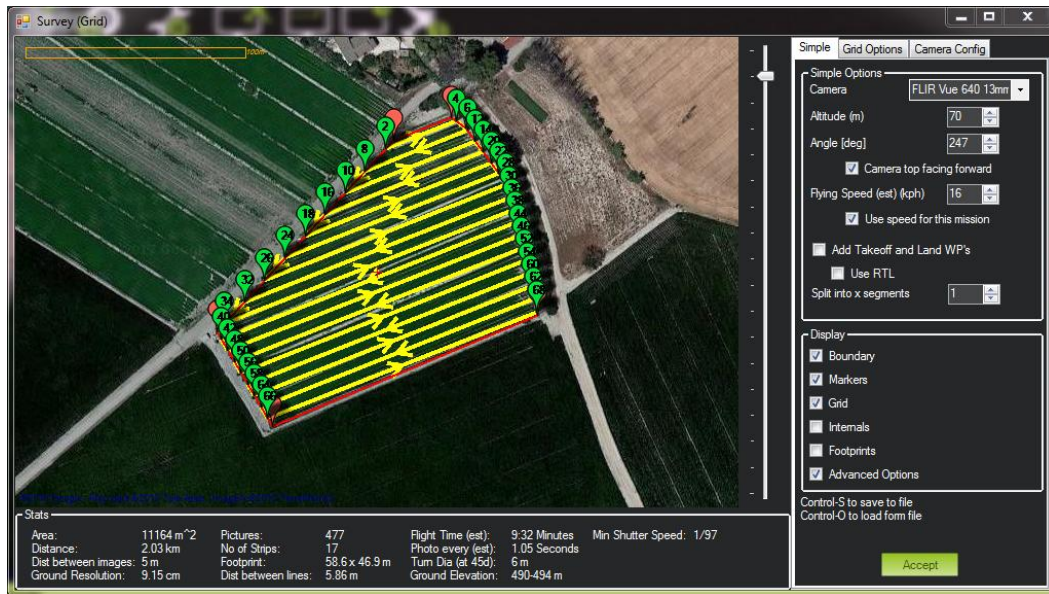


Figure 17. Stepped down aircraft speed to meet the requirement of 1s between shots.

Decreasing the aircraft speed to 16 km/h will allow triggering the camera at a rate of 1,05s. Figure 17 also shows the final flight time after the speed modification. It is important to check if the new flight time is lower than the maximum flight time of the aircraft. In this case, a flight time of 9:32 minutes will be far from reaching the ~19 min@16 km/h flight time limit. The new flight distance will remain under the ~4,5km@16 km/h simulated.

5 Flight performance at field

The RPAS was subjected to field test flights to ensure that all of the on-board integrated systems were working. The flight tests presented in the frame of the T3.3 were done on August 11 and October 26, 2017. Over 60 flights have been done with the aircraft.

5.1 Flight procedure and warning situations

During the flight tests, the operator applied the following flight procedure:

1. The GCS must be in place and in good working conditions. The multicopter is set in place and the battery is connected.
2. The GCS will connect with the aircraft through the telemetry link in order to check the telemetry, to send the configuration flight parameters and to start the aircraft status monitoring.
3. With the GCS connected through the telemetry link, it is the moment to send the flight plan already prepared to the RPA.
4. A preflight checklist must be rigorously passed before the arming of the motors.
5. If all the flight instruments are operative (EKF and Vibe alerts off), the GPS is available, the radio transmitter is on and available, the checklist has been passed and the takeoff area is clear from persons and animals, the operator can proceed with the aircraft arming then the arming of the motors.
6. Although the aircraft is auto takeoff and landing capable, it is preferable that the operator takes off manually until the target altitude then switch to auto mission mode.
7. During the auto mission, the operator must monitor the status of the aircraft at all moment without losing the line of sight with the aircraft. It is especially important to check the battery voltage, the total drive current consumption (especially in windy conditions that causes current peaks) and the percentage of remaining battery. A sound warning is activated when a critical threshold is reached.
8. After the mission, the aircraft returns to home (the take-off place). It is preferable that the landing is also performed manually rather than automatically.

Warning:

- If the air temperature is under 10°C, the battery can have worse performances. Consider to preheat the battery and to avoid heavy battery demanding missions.
- The loss of the telemetry link depends on the GCS and air segment telemetry setups but as standard, the signal is lost between 500 m and 700 m if there is a clear line of sight. In other conditions the loss of signal can occur before.
- The transmitter control radio link usually shows a signal loss between 800 m and 1 km if there is a clear line of sight. As in the case of the telemetry link, in other conditions, the loss of signal can occur before.

5.2 Flight performance during the two test flights

The two test flights were driven over a field of 1,12 ha with a time separation of two months.

During the two test flights we had absolutely any problem.

Date	Real area covered (ha)	Altitude AGL (m)	Flight time (min)	Weather conditions	Const./max. total drive current (A)	Cruise ground speed (km/h)	Initial battery charge (%)	Final battery charge (%)	Max. distance to home (m)	Payload
11/08/2017	2,64	70	12:33	23°C, RH: 65%, no wind, no clouds	26/29	14-16	99	42	140	Multi + TIR

Table 10. Flight performance of the first test flight.

Date	Real Area covered (ha)	Altitude AGL (m)	Flight time (min)	Weather conditions	Const./max. total drive current (A)	Cruise ground speed (km/h)	Initial battery charge (%)	Final battery charge (%)	Max. distance to home (m)	Payload
26/10/2017	2,76	70	12:54	20°C, RH:55%, no wind, no clouds	26/30	14-16	99	39	140	Multi + TIR

Table 11. Flight performance of the second test flight.

It is important to mention that although the field was 1,12 ha, the camera with the lower focal length (Micasense RedEdge 3) covered more than twice the area of interest. This will ensure a very good overlap all over the interest area.

In both flights the movement when in auto mission mode was very smooth and the ground speed slightly slower than the specified during the mission planning. This speed difference is due to the fact that the flight follows a grid pattern and not a line. Each time the aircraft approaches a waypoint, the speed decreases. The speed recover after a waypoint visit is slow.

The auto takeoff and landing are avoided as the climb rate of the aircraft in auto mode is low in order to assure stability. Taking off and landing in manual mode saves flight time and is considered safer.



5.3 Relevant incidents occurred during other flights of the aircraft

During the rest of the flights, we experimented a telemetry loss because of the loss of line of sight between the GCS and the aircraft due to a mass of trees with the GCS, a thermal camera geo-referencing loss due to a bug in the camera firmware (v2.1.2) which was later solved by the manufacturer.

6 Preliminary data analysis

Two sets composed of multispectral and TIR data were acquired over the test field with a separation of two months with the aim of visualizing vegetation differences. This data will be used as a starting point to evaluate the processing pipeline together with the data acquired along the T3.1 by ONERA.

6.1 Photogrammetric software

The selected software to drive the preliminary data processing and analysis is Pix4D. The principal advantage of this software over others in the market is that it carries out all the processing steps necessary to process raw images until the generation of reflectance, indices and temperature orthomosaics.

When images are loaded to a Pix4D project, they are represented in the map by red points united by a flight path. Figure 18 shows the number of triggers in the cases of the multispectral camera and the thermal infrared camera. The overlap is higher (90%) in the TIR case than in the multispectral (80%) case. We can appreciate this in the higher red point density of the TIR case in the right side of the image.



Figure 18. Multispectral (left) and TIR (right) flight paths with camera triggers.

Figure 19 shows the processing pipeline in three steps of Pix4D.

When starting *Initial Processing*, Pix4D first computes keypoints (descriptors) in the images. It uses these keypoints to find matches between the images. From these initial matches, the software runs an Automatic Aerial Triangulation (AAT) and Bundle Block Adjustment (BBA). If the initial processing has already been done and is restarted, the software uses the existing keypoints and matches and starts the AAT and BBA. If from one processing to

another the project type has changed, additional matches might be computed as the matching procedure is different for each project type.

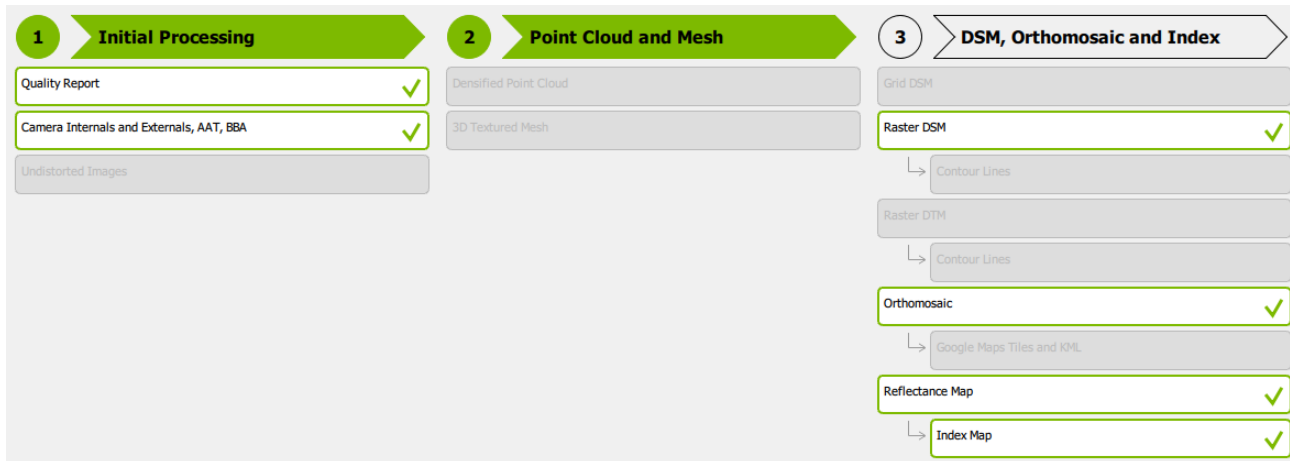


Figure 19. Pix4D output status diagram showing the complete processing pipeline.

The *Point Cloud and Mesh* will build on the Automatic Tie Points with:

- Point Densification: Additional Tie Points are created based on the Automatic Tie Points that results in a Densified Point Cloud.
- 3D Textured Mesh: Based on the Densified Point Cloud a 3D Textured Mesh can be created.

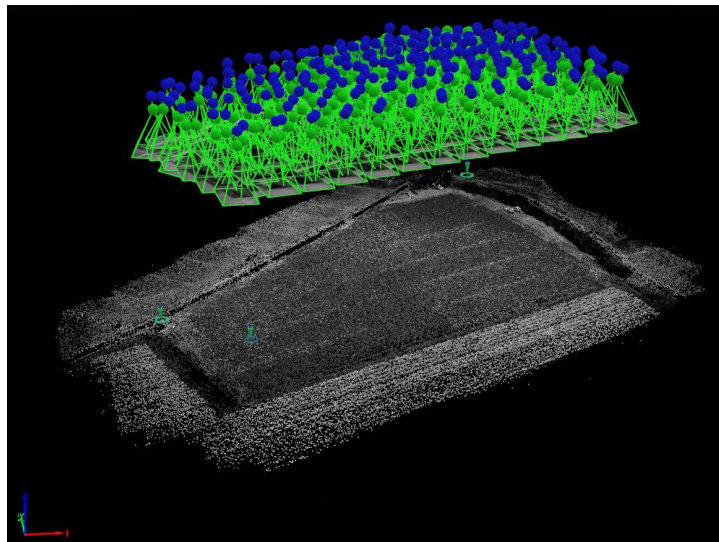


Figure 20. Raycloud editor.

Figure 20 shows the densified point cloud of the Raycloud, which allows the visualization of the different elements of the reconstruction (Camera Positions, Reprojections (rays), GCPs, Manual / Automatic Tie Points, Processing Area, Clipping Box, Densified Point Cloud, Point Cloud Classification, 3D Textured Mesh, Video Animation Trajectories) and their properties.

When the flight has been done without the presence of wind, the miniature pictures in the 3D View window of the Raycloud appear mostly horizontal. In presence of wind the multicopter has to increase the tilt angle to maintain the progress of the aircraft and the miniature pictures in the 3D View window of the Raycloud appear mostly oblique.

The final step *DSM, Orthomosaic and Index* enables the creation of:

- Digital Surface Model (DSM): The creation of the DSM will enable the computation of Volumes, Orthomosaics and Reflectance Maps.
- Orthomosaic: The creation of the Orthomosaic is based on orthorectification. This method removes the perspective distortions from the images.
- Reflectance Map: The goal is to produce a map where the value of each pixel faithfully indicates the reflectance of the object (the reflectance map is only generated if the spectralon images calibration process is done and the downwelling light sensor is installed).
- Index Map: Generate an Index Map where the color of each pixel is computed using a formula that combines different bands of the Reflectance Map(s).

6.2 Processing quality report

The quality of the generated orthomosaic will depend mainly on the number of keypoints found per image. The number of keypoints increases by increasing the overlap.

Summary



Project	Pix4D-Multispectral
Processed	2017-11-12 21:53:19
Camera Model Name(s)	RedEdge_5.5_1280x960 (Blue), RedEdge_5.5_1280x960 (Green), RedEdge_5.5_1280x960 (Red), RedEdge_5.5_1280x960 (NIR), RedEdge_5.5_1280x960 (Red edge)
Rig name(s)	«McaSense 5 band»
Average Ground Sampling Distance (GSD)	4.55 cm / 1.79 in
Area Covered	0.0262 km ² / 2.6246 ha / 0.0101 sq. mi. / 6.489 acres
Time for Initial Processing (without report)	45m:49s

Quality Check










 Images	median of 10000 keypoints per image	
 Dataset	1320 out of 1320 images calibrated (100%), all images enabled	
 Camera Optimization	0.79% relative difference between initial and optimized internal camera parameters	
 Matching	median of 5718.3 matches per calibrated image	
 Georeferencing	yes, no 3D GCP	

Table 12. Pix4D Quality Report Summary.

Table 12 shows the summary of the orthomosaic generation process extracted from the quality report made by Pix4D during the *Initial Processing* step. In this summary we can find important information like the area covered or the average GSD. There are also some quality check parameters like the median of keypoints per image, the number of calibrated images, the relative difference between the initial and optimized camera parameters or the median of matches per image.

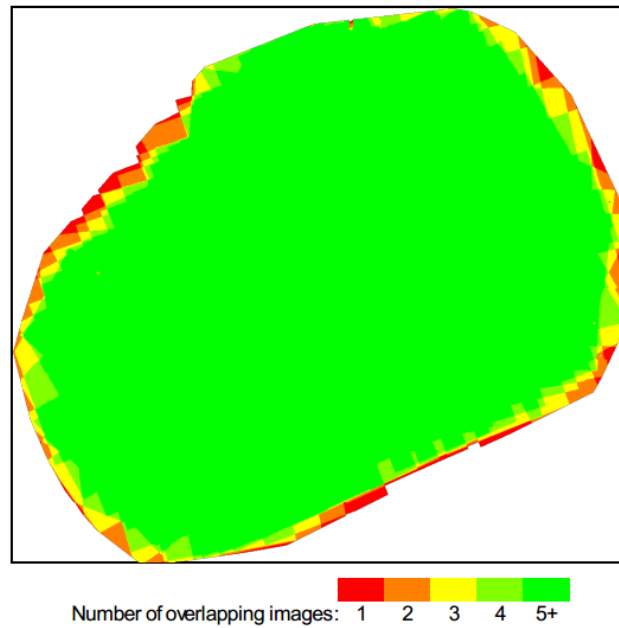


Figure 21. Spatial color representation of the number of overlapping images.

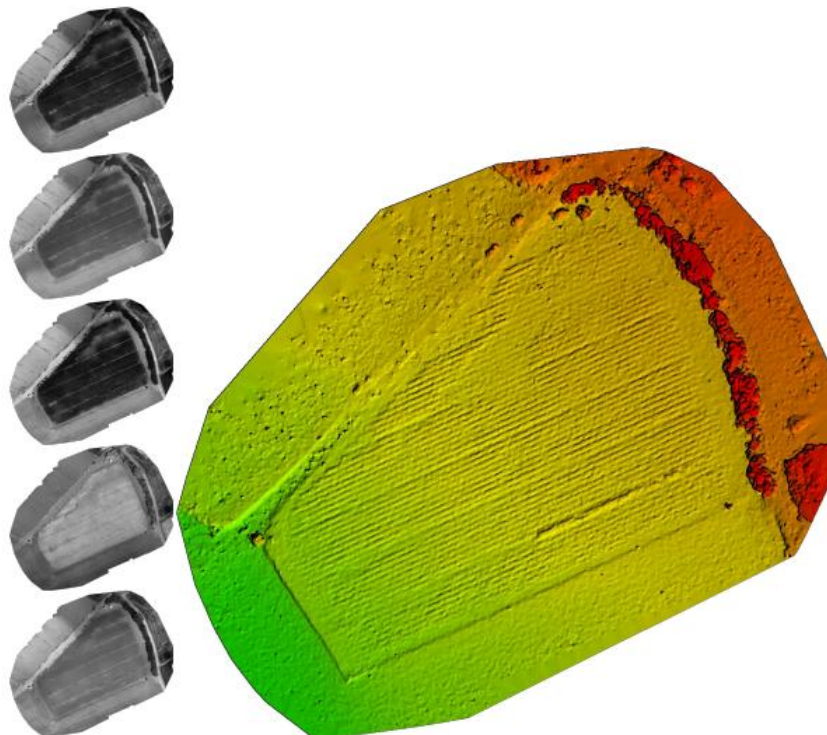


Figure 22. Quick view of the spectral bands and the computed DSM.

Figure 21 shows a color spatial representation of the number of overlapping images. The green color indicates that the selected overlap was enough to compute a quality orthomosaic.

The quality report includes a quick view of the spectral orthomosaics and the computed DSM as seen in Figure 22.

6.3 Generated orthomosaic

Figure 23 shows the linear contrast representation of the spectral reflectance (reflectance in the processing pipeline after the calibration with spectralon images and the downwelling light 5 bands data acquired for each image) and brightness temperature (assuming emissivity is 1) orthomosaics. All the bands are co-registered. It is possible to appreciate slightly differences between the mosaics but the image interpretation remains difficult.

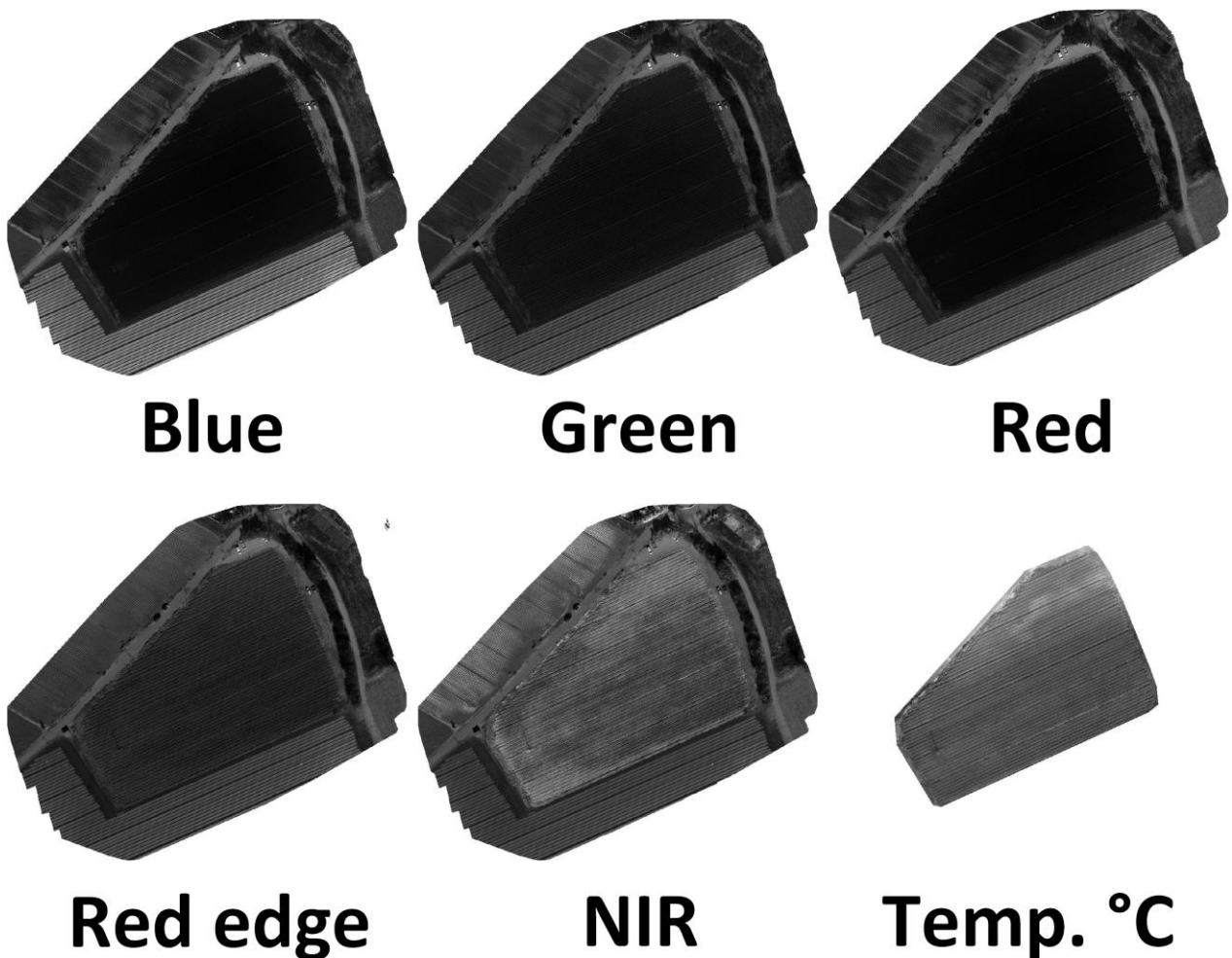


Figure 23. Comparison between the spectral reflectance and brightness temperature orthomosaics.

Figure 23 is only a qualitative preview. The rest of the generated orthomosaics is not shown here as the difficulty of interpretation makes over any interest. To increase significantly the interpretation interest, additional processing steps like the Cartesian representation of its pixels in the space NIR-R (explained and covered in D3.1) or the computing of algebraic specific indexes are needed.

6.4 Sample indices

The computing of algebraic indexes makes easier the interpretation of spectral data. Moreover when comparing time series like in this case. The data acquired and processed in the two test flights have been represented by means of algebraic spectral indexes. The two indexes selected for representing the test data are the NDVI (Normalized Difference Vegetation Index) and the ARI (Anthocyanin Reflectance Index).

$$NDVI = \frac{(NIR - Red)}{(NIR + Red)}$$

$$ARI1 = \frac{1}{\rho_{550}} - \frac{1}{\rho_{700}}$$

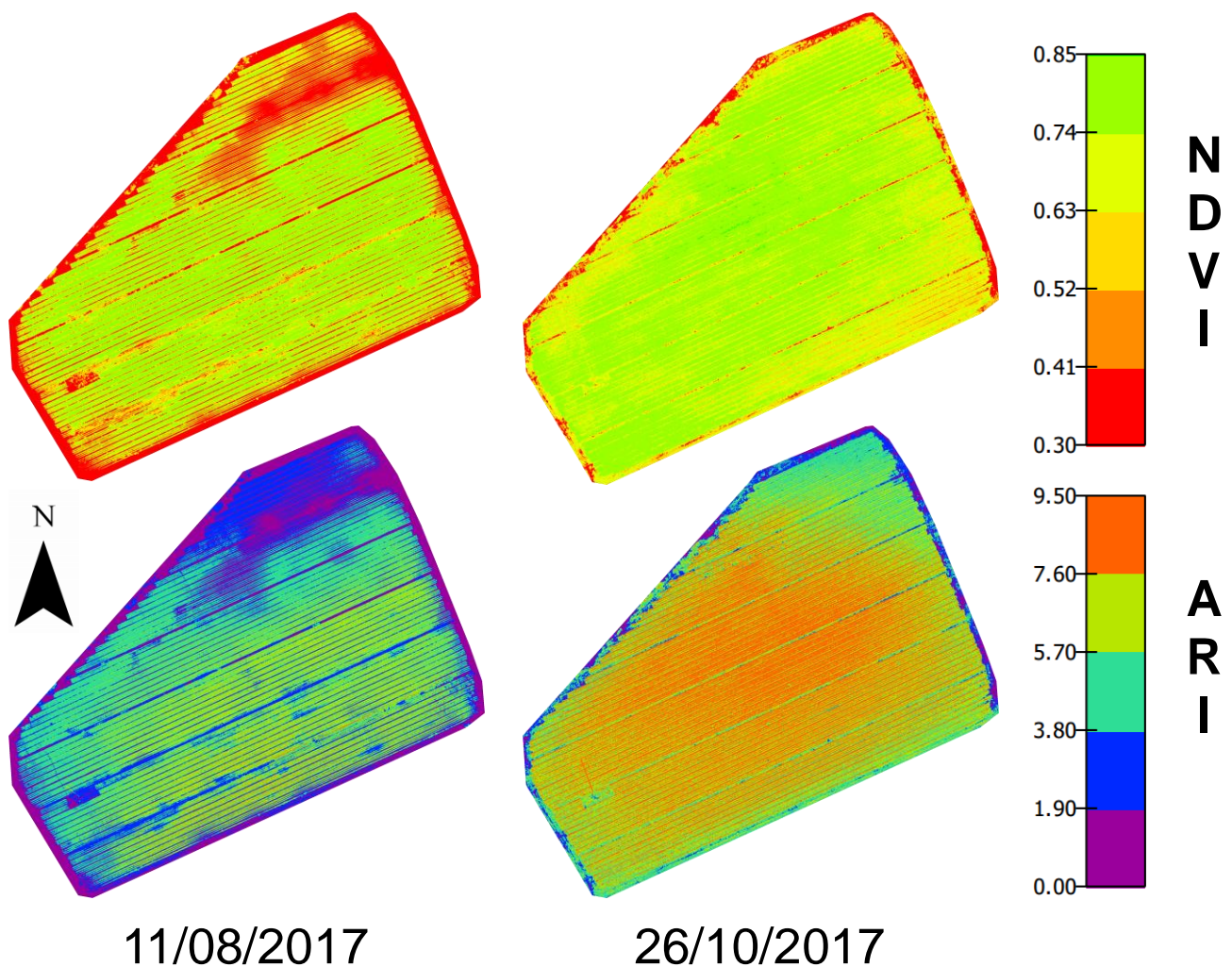


Figure 24. Study of the evolution of the greenness and the anthocyanin leaf content of a carrot crop test field.

The NDVI plots of the Figure 24 shows an expected increase of greenness due to the plants growth with a proper irrigation over the two months period (BBCH 76 – BBCH 79 respective phenological stages). However, the picture shows an intra-plot variability probably due to the soil characteristics variability or even an unequal irrigation.

The anthocyanin index [3] shows a drastic increase of the amount of the anthocyanin leaf content which in this case is due to the attack of the Candidatus phytoplasma bacterium.

This indices have been selected as a sample of the application capabilities.

Regarding the orthomosaic generated from the thermal camera, it has been considered to represent the brightness temperature orthomosaic and the CWSI (Crop Water Stress Index) obtained by an approximation to the empirical method established by Idso in 1981 [4].

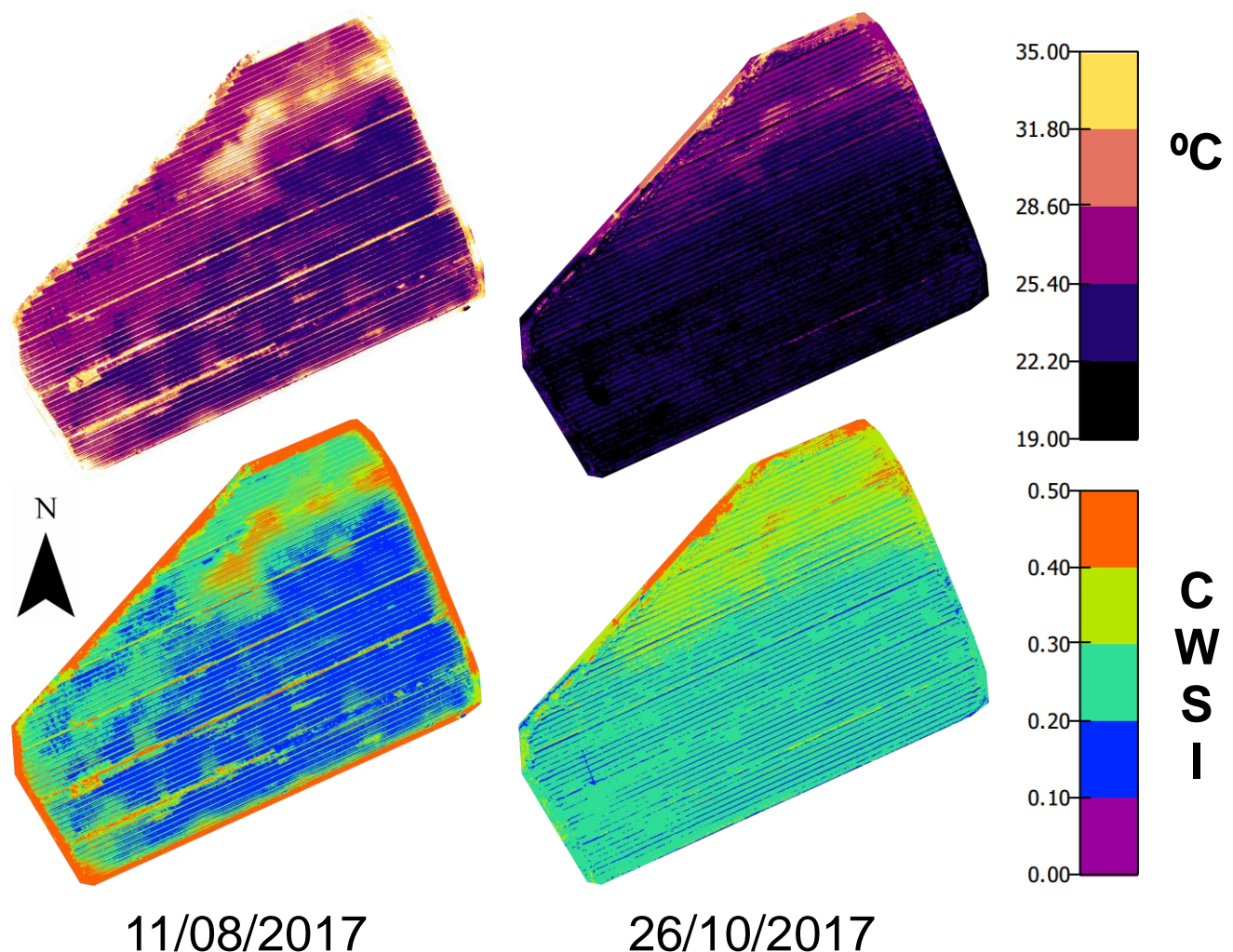


Figure 25. Study of the evolution of the temperature and the water stress in the carrot crop test field.

The temperature decrease over the two flights showed in the Figure 25. There are many potential reasons for a temperature decrease as for example different environment conditions (air temperature, solar flux, wind, ...) and transpiration, but also to the increase of the carrot leaves which cover a greater soil fraction.

The CSWI suggests a lack of irrigation in the last period. The variability in the CSWI over the two periods suggests that maybe the field has a slight inclination or possibly a variation in the soil composition that affects the soil drainage. The CWSI is more uniform in the last period although we appreciate the same CWSI homogeneous areas than in the first period.

7 Conclusions

The calculation and simulation tool has been found true to reality. The aircraft simulated performance is very close to the performance in real flight conditions. The use of this kind of calculation and simulation tools is a must in any UAV design process.

After the aircraft simulation and test process we conclude that the implemented multicopter is a suitable candidate to fulfill the WADI project needs. The difference between simulated and real conditions have been considered in the design process. The result has been an aircraft conservative regarding safety of flight while not being oversized. It has been proven a flight platform stable, operating safely away from its maximum ratings and capabilities.

There is not a wide UAV sensor market to make a selection based on features comparison. The integrated UAV payload is composed by the best in its class UAV sensors in the market. Both cameras fulfill the spectral and operational needs of the WADI project.

The presented index examples are only a demonstrator of the system's capability. The indices have been calculated from the spectral reflectance orthomosaics where the reflectance has been calculated after the calibration process based on spectralon images and downwelling light spectral sensor data acquired at each multispectral camera trigger (each image has an associated downwelling light value).

The indices should be computed with reflectance values, not radiance nor "raw" signal values. Otherwise, there is a bias. However, for the purpose of the triangle method presented in D3.1 such a bias is not a great problem. In some way, since we use NDVI or OSAVI in a relative sense (not absolute sense), this bias is not a problem at all. The ease of the reflectance calibration process in the UAV case contrasts with the difficulty to calibrate airborne images (long flights, absence of spectralon calibrated images and downwelling light sensor), so the triangle method is a keypoint common to both aerial platforms.

The photogrammetric software Pix4D has been found useful for driving all the image processing steps until the algebraic indices calculation. The whole processing with Pix4D takes 15 to 60 minutes per flight of 20 ha. The raw spectral, spectral reflectance, brightness temperature and calculated indices' orthomosaics remain perfectly co-registered. PIX4D will be a candidate for the WADI data processing developed in WP4.

8 References

- [1] Markus Müller. (2018). *xcopterCalc*. Last visit: March 7, 2018, <https://www.ecalc.ch/>.
- [2] Pix4D (2018). How are the internal and external camera parameters defined. Last visit: March 7, 2018, <https://support.pix4d.com/hc/en-us/articles/202559089-How-are-the-Internal-and-External-Camera-Parameters-defined->
- [3] Gitelson, A., M. Merzlyak, and O. Chivkunova. (2001) Optical Properties and Nondestructive Estimation of Anthocyanin Content in Plant Leaves. *Photochemistry and Photobiology* 71: 38-45.
- [4] Idso, S.B.; Jackson, R.D.; Pinter, P.J., Jr.; Reginato, R.J.; Hatfield, J.L. (1981) Normalizing the stress-degree-day parameter for environmental variability. *Agric. Meteorol.* 24: 45–55.